applied sciences

MDPI

Article

Experiments on Material Proportions for Similar Materials with High Similarity Ratio and Low Strength in Multilayer Shale Deposits

Yaobin Shi [1,2,3], Yicheng Ye [1,2,3], Nanyan Hu [1,2,*], Xu Huang [1] and Xianhua Wang [4]

1 School of Resource and Environmental Engineering, Wuhan University of Science and Technology, Wuhan 430081, China; shiyaobin@wust.edu.cn (Y.S.); yeyicheng@wust.edu.cn (Y.Y.); drift_alone@163.com (X.H.)
2 State Environmental Protection Key Laboratory of Mineral Metallurgical Resources Utilization and Pollution Control, Wuhan University of Science and Technology, Wuhan 430081, China
3 Hubei Key Laboratory for Efficient Utilization and Agglomeration of Metallurgic Mineral Resources, Wuhan University of Science and Technology, Wuhan 430081, China
4 Sinosteel Wuhan Safety and Environmental Protection Research Institute Co., Ltd., Wuhan 430081, China; ssriwangxh@163.com
* Correspondence: hunanyan@wust.edu.cn

Citation: Shi, Y.; Ye, Y.; Hu, N.; Huang, X.; Wang, X. Experiments on Material Proportions for Similar Materials with High Similarity Ratio and Low Strength in Multilayer Shale Deposits. *Appl. Sci.* **2021**, *11*, 9620. https://doi.org/10.3390/app11209620

Academic Editor: Giuseppe Lacidogna

Received: 4 October 2021
Accepted: 14 October 2021
Published: 15 October 2021

Abstract: It is important to systematically investigate the similar materials with high similarity ratio and low strength in multilayer shale deposits, to provide a scientific basis and experimental basis for the research of underground mining of multilayer shale deposits. In this paper, using an orthogonal experimental method, the physical and mechanical parameters of different material proportions were analyzed with four control factors of mica powder/standard sand, filling material/bonding material, Portland cement/gypsum, silicone oil ratio. Twenty-five groups of material proportioning schemes were designed, and the density, porosity, compressive strength, and elastic modulus of each group of materials were measured. Through the range analysis and significance analysis, the influence of control factors on the material parameters was explored, and multivariate linear regression analysis of test results was carried to eliminate outliers. The result showed that the physical and mechanical parameters of similar materials prepared according to the proportioning scheme were widely distributed, which can meet the preparation requirements of similar materials with different lithologies. The density and compressive strength were most affected by the ratio of Portland cement/gypsum, the porosity was most affected by the ratio of filling material/bonding material, and the elastic modulus was mainly controlled by the silicone oil ratio. The proportioning scheme was applied to three similar prepared shale materials with large lithology differences. The error between actual similar constant and design similar constant of low strength similar material was less than 1.62%. The physical and mechanical parameters of similar materials were in good agreement with the original rock.

Keywords: similar materials; orthogonal experimental design; proportioning test; low strength similar materials; shale

1. Introduction

The physical similarity simulation test is an important, effective, and scientific research method to solve complex geotechnical engineering problems [1–3]. Choosing suitable similar materials, which are according to the properties of the simulated prototype material, is the basis of physical similarity simulation test, to truly reproduce the physical entity and reflect the basic physical and mechanical properties of geotechnical media [4,5]. Similar material simulating geotechnical mechanical properties must have the basic characteristics of high gravity, low strength, low deformation modulus, and variable internal friction angle. Materials that meet these requirements do not exist in nature and must be combined manually [6,7]. In sum, selection and proportioning of similar materials play a decisive role in the physical similarity simulation test [8,9].

In the large-scale geotechnical engineering similarity simulation experiment, the biggest difficulty is the reduction and simulation of the actual discontinuity and low-strength rock (rock stratum). Similar materials with high similarity ratio, low strength, and high adaptability are difficult to mix and prepare their models [10,11]. Scientists and technicians have made many achievements in the study of discontinuities, similar materials, and similar models of low-strength rocks. In this context, Zilong XU and co-workers [12] composed the similar material of surrounding rock by using quartz sand as coarse aggregate, barite powder as fine aggregate, and oil, Vaseline, and paraffin as binder. Physical and mechanical parameters such as uniaxial compressive strength, elastic modulus, and cohesion of materials were controlled through uniaxial compressive, direct shear, and splitting tests. They systematically studied the influence laws of mechanical parameters under various ratios and explored the mechanism of crack damage of long-span tunnel lining and the variation rules. Fu H.Y. et al. [13] developed similar materials for silty mudstone, which has characteristics of low strength and water expansion, based on traditional materials including gypsum, barite powder, clay minerals, and distilled water. They used the orthogonal design method to determine the mixing ratios of the similar materials, and selected the density, uniaxial compressive strength, tensile strength, elastic modulus, and Poisson's ratio as control indicators of the similar materials. Sun Peng et al. [14] selected pulverized coal as aggregate, sodium humate as cementing agent, and river sand as auxiliary materials, obtaining the similar materials with specific physical and mechanical parameters and adsorption and desorption indexes used in coal and gas outburst simulation tests. They designed orthogonal tests with six factors and five levels, and carried out the tests of weighing, uniaxial compression, firmness, adsorption and desorption. The parameters such as density, uniaxial compressive strength, elastic modulus, firmness coefficient, and adsorption–desorption index of similar materials with different ratios were obtained, and the sensitivity of each factor was analyzed by range analysis.

The research should identify which study of similar material model is one of the effective means to reveal the relationship between discontinuity and rock mass performance and to study the geotechnical engineering in discontinuity. However, there are few studies on the proportion and model of low-strength similar materials with high geometric similarity ratio (uniaxial compressive strength less than 2 MPa) [15–18]. Therefore, it is necessary to further study the similarity simulation model of low-strength similar materials and large-size, high geometric similarity ratio of multi-layer shale deposits by using environmentally friendly, low-cost, and effective similar materials, which are very necessary for the physical similarity simulation test and underground mining research of this kind of deposit.

In this paper, the proportioning test of similar materials was designed based on the similarity principle. The Shanghengshan multi-layer shale deposit was taken as the research object, and sand, glycerol, gypsum, iron ore powder, and mica powder with low cost and being environmentally friendly were used as the basic materials. The physical and mechanical parameters of different material proportions were analyzed with four control factors of mica powder/standard sand, filling material/bonding material, Portland cement/gypsum, and silicone oil ratio, and designed with five different gradients (five levels). Twenty-five groups of similar test proportions were designed based on the principle of the orthogonal test. Through the proportion test of similar materials, the influencing factors of various physical and mechanical indexes were analyzed, and the multiple linear regression analysis of removing abnormal points was carried out to determine the appropriate proportion of similar materials. Combined with the occurrence conditions and exploration conditions of geotechnical engineering, a large-scale physical similarity model was made. This study can not only provide a basis for the actual similarity simulation research but also serve as a scientific basis for the study of high similarity ratio and low-strength similar materials' proportioning.

2. Design of Similar Material Proportioning Test Scheme

2.1. Similarity Test Design

There are three main aspects in the test of simulating similar materials of ore and rock mass instead of the prototype rock mass. Firstly, the sensitivity test is carried out by a uniform design method to prepare samples of similar materials [19,20]. Secondly, the engineering rock mass test and geotechnical test are used to test the samples of similar materials, measure the physical and mechanical property parameters of the samples, and analyze and compare the relationship between different sand binder ratio, cement content in cementitious materials, and the properties of similar materials. Finally, based on the similarity principle, the physical and mechanical parameters of similar materials are determined. Combined with the engineering research object, a similar material model is made to verify the effectiveness of similar materials.

The method and procedure of the proportioning test of similar materials are shown in Figure 1.

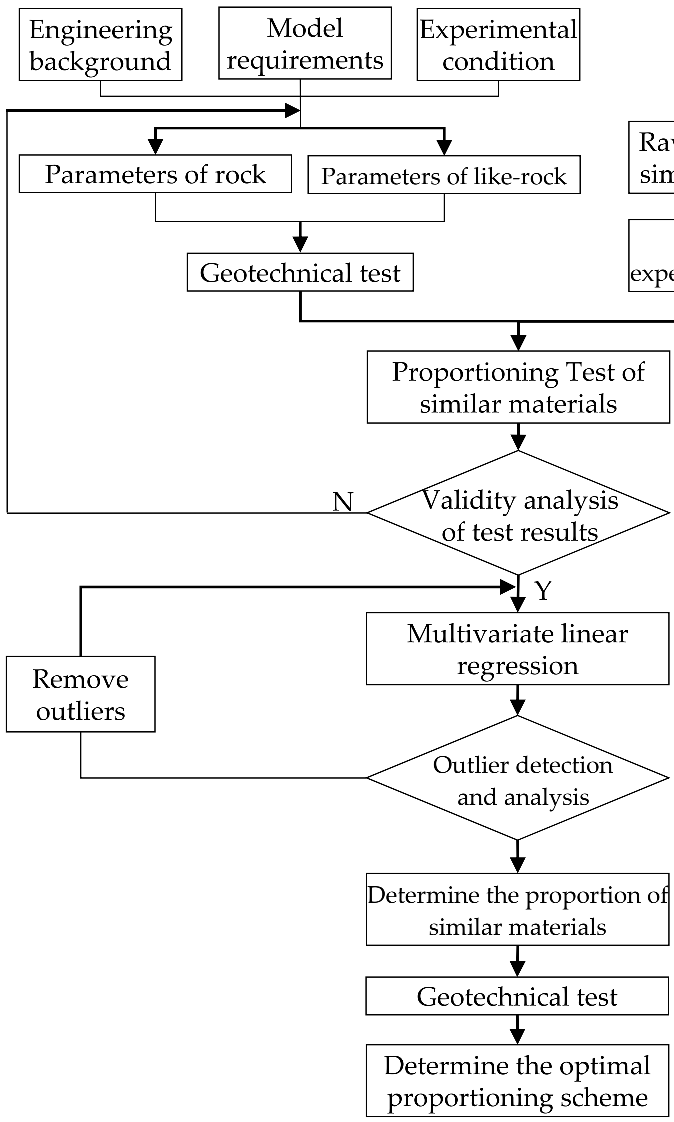

Figure 1. Flow chart of determining the similar material proportion.

2.2. Similarity Test Similarity Principle

Selecting appropriate model materials in the physical simulation test is one of the key links of quantitative simulation [21,22]. Similar materials and raw model materials need to follow similarity criteria, determining their similarity conditions according to the characteristics of the research object, meeting the similarity in geometric characteristics, physical and mechanical properties, deformation characteristics, etc. of similar materials [23,24]. The similarity model and prototype should meet the similarity conditions in the structure and its failure characteristics, boundary conditions, elastic–plastic stress state, time, etc. [25–27].

According to the physical and mechanical characteristics and simulation conditions of ore and rock mass, the following similarity relationship is deduced through dimensional analysis:

$$C_\varepsilon = C_\mu = C_\varphi = C_n = 1$$

$$C_\sigma = C_E = C_c = C_{\sigma_c}$$

$$\frac{C_\sigma}{C_\rho C_l} = 1$$

where C_ε, C_μ, C_φ, C_n, C_σ, C_E, C_c, $C_{\sigma c}$, C_ρ, and C_l are the similarity ratio of strain, Poisson's ratio, internal friction angle, porosity, stress, elastic modulus, cohesion, compressive strength, density, and geometry.

In this study, the dimensionless parameters such as Poisson's ratio, porosity, and internal friction angle of similar materials were selected, and the similarity constant was 1. The determined geometric similarity constant C_l was 100, and mechanical similarity constants mainly included bulk density (density) and stress similarity constants, C_ρ is 1.5 and C_σ is 150, respectively.

2.3. Orthogonal Experimental Design

In the proportion of similar materials, the water consumption in the test was 10% of the total mass of the materials used. Therefore, the L25 (4^5) (four factors and five levels) orthogonal design test was selected for the Proportioning Test of similar materials [28]. The orthogonal scheme is shown in Table 1, and the proportioning scheme of similar materials under different test conditions is shown in Table 2.

Table 1. Orthogonal design table of similar materials.

#	1	2	3	4
Factor	**Mica Powder/Standard Sand**	**Filling Material/Bonding Material**	**Portland Cement/Gypsum**	**Silicone Oil Ratio/%**
1	0	6:1	3:7	0
2	0.25	7:1	4:6	2.5
3	0.50	8:1	5:5	5.0
4	0.75	9:1	6:4	7.5
5	1	10:1	7:3	10.0

Table 2. Test schemes of material proportions.

#	Mica Powder/Standard Sand	Filling Material/Bonding Material	Portland Cement/Gypsum	Silicone Oil Ratio/%
1	0	6:1	3:7	0.0
2	0	7:1	4:6	2.5
3	0	8:1	5:5	5.0
4	0	9:1	6:4	7.5
5	0	10:1	7:3	10.0
6	0.25	6:1	4:6	5.0
7	0.25	7:1	5:5	7.5
8	0.25	8:1	6:4	10.0
9	0.25	9:1	7:3	0.0
10	0.25	10:1	3:7	2.5
11	0.50	6:1	5:5	10.0
12	0.50	7:1	6:4	0.0

Table 2. *Cont.*

#	Mica Powder/Standard Sand	Filling Material/Bonding Material	Portland Cement/Gypsum	Silicone Oil Ratio/%
13	0.50	8:1	7:3	2.5
14	0.50	9:1	3:7	5.0
15	0.50	10:1	4:6	7.5
16	0.75	6:1	6:4	2.5
17	0.75	7:1	7:3	5.0
18	0.75	8:1	3:7	7.5
19	0.75	9:1	4:6	10.0
20	0.75	10:1	5:5	0.0
21	1.00	6:1	7:3	7.5
22	1.00	7:1	3:7	10.0
23	1.00	8:1	4:6	0.0
24	1.00	9:1	5:5	2.5
25	1.00	10:1	6:4	5.0

3. Proportioning and Test Preparation of Low-Strength Similar Materials

3.1. Simulation Prototype of Proportioning Test of Similar Materials

This paper studied the mining project of the Shanghengshan multi-layer shale deposit. There are 12 ore bodies in the ore section. The ore bodies are produced in layers, with good continuity and simple shape. The ore-bearing rocks are mainly carbonaceous shale, siliceous shale, and Vanadium-bearing shale, followed by siliceous rock. The ore body has a dip of 150°~220° and an inclination of 5°~25°. The ore length is 615~952 m, the thickness is 0.75~7.27 m, the thickness variation coefficient is 37.07~64.59%, and the inclined extension depth is 103~223 m. Considering the deposit occurrence conditions and physical similarity simulation conditions, the physical and mechanical parameters of ore and rock mass are shown in Table 3 [21].

Table 3. Mechanics' parameter of model materials.

Rock Formation	Density /(kg/m^3)	Compressive Strength /MPa	Tensile Strength /MPa	Elastic Modulus /GPa	Poisson's Ratio	Cohesion /MPa	Internal Friction Angle /(°)
Siliceous shale	2564.72	112.63	17.24	59.8	0.21	10.7	41.0
Vanadium-bearing shale	2482.53	76.69	12.56	58.8	0.21	9.3	40.4
Carbonaceous shale	2429.86	49.45	7.42	50.8	0.20	8.5	40.0

The engineering geological drilling of the Shanghengshan deposit showed that the stability of the bottom layer of multi-layer gently inclined shale is poor, resulting in increased mining risk of underground deposit. Therefore, the actual geological conditions of the Shanghengshan gently inclined multi-layer deposit can be restored to the greatest extent through indoor simulation experiments, and the mining methods and schemes are designed and optimized according to the underground geotechnical environment of the deposit. Accordingly, to truly represent the geological conditions of the gently inclined multi-layer shale formation of the Shanghengshan deposit, it was necessary to build a large-scale, high similarity ratio, and low-strength indoor physical similarity simulation model with matching similar materials.

3.2. Raw Material Selection of Similar Materials

In the physical simulation test, selecting the appropriate model materials is one of the key links of quantitative simulation. In the laboratory, similar materials are used to develop the proportion of similar materials according to the similarity principle. The internal force parameters, deformation state, and stress distribution law of the model are observed with the help of the test instrument. We inferred the possible mechanical phenomena in the prototype according to the research results on the model, so as to use the research of a similar model to solve the practical problems in production. For this purpose, the following requirements must be met for similar materials.

- The main mechanical properties of similar materials should be similar to the structure of simulated rock stratum.
- The mechanical properties of the material are stable and not easy to be affected by external conditions, such as temperature, humidity, etc.
- Changing the ratio of materials can change the mechanical properties of materials to meet the needs of similar conditions.
- Similar materials are easy to form, easy to manufacture, and have a short solidification time.
- A wide source of materials with low cost is necessary.

According to the current scholars' research on rock similar materials, combined with the research of gypsum similar materials and mortar similar materials (Chen Shaojie, et al., 2015 [29]; Li Jian Guang, et al., 2017 [30]; Lin Manqing, et al., 2020 [31], Ko Tae Young, et al., 2020 [32]), standard sand and mica powder were selected as filling materials, Portland cement and gypsum as the binder, and silicone oil and water as the regulator. Among them, gypsum passed through 120 target standard sieves, and the sieve residue was less than or equal to 0.2%. C32.5 Portland cement was selected for cement, and the particle size of river sand was less than or equal to 12 mesh.

3.3. Matching Process of Similar Materials

According to the provisions of the test method for mechanical properties of ordinary concrete [33] and the code for rock test of water resources and Hydropower Engineering [34], standard specimens with a diameter of 50 mm and a height of 100 mm were selected for the test.

Firstly, the cementitious materials and filling materials were weighed according to the specified ratio and poured into the container for full mixing. Water and glycerol were added for further mixing. The mixed materials were poured into the steel test mold, and the hydraulic universal pressure tester was used for mechanical compaction (forming pressure 6 MPa). Then, the formwork was removed after being placed in the room under constant temperature and humidity for 3 days. The label was pasted onto the surface of the sample, and then placed in the room under constant temperature and humidity for drying for 25 days. Samples of similar materials cured at room temperature are shown in Figure 2, and Samples of similar materials after the test are shown in Figure 3.

Figure 2. Sample of similar material.

(a) (b)

Figure 3. Uniaxial mechanical test of similar materials. (**a**) Uniaxial compression test. (**b**) Sample after mechanical test.

4. Test Results and Analysis

4.1. Applicability Analysis of Similar Materials

In combination with the needs of a later physical similarity simulation test, a mineral material density instrument was used to test the density, a porosity instrument was used to test the porosity, and a rock uniaxial instrument was used to test the parameters such as compressive strength and Poisson's ratio. After testing, the density, porosity, compressive strength, and elastic modulus of each group of samples were obtained. The specific results are shown in Table 4. According to the physical and mechanical parameter requirements of this similar model test, the material ratio that meets or approximately meets the similar requirements can be selected from the orthogonal test results.

Table 4. Experimental results of material proportions.

#	Density/ $(kg \cdot m^{-3})$	Porosity/ %	Compressive Strength/ MPa	Elastic Modulus/ GPa
1	1769.78	14.53	0.31	0.3394
2	1802.30	15.16	0.76	0.3868
3	1742.15	16.88	0.90	0.4273
4	1746.55	14.46	0.51	0.3944
5	1808.40	14.24	1.43	0.4092
6	1776.02	15.72	0.46	0.3569
7	1726.02	13.64	1.05	0.4454
8	1812.17	14.15	1.38	0.3992
9	1768.26	13.45	0.65	0.3824
10	1684.64	18.56	0.33	0.3268
11	1726.02	13.64	1.05	0.4454
12	1821.49	11.52	1.16	0.4007
13	1779.40	13.96	1.03	0.4064
14	1708.60	17.88	0.64	0.3807
15	1727.05	18.07	0.69	0.3762
16	1846.92	10.12	2.23	0.4168
17	1800.93	11.68	1.66	0.4460
18	1709.41	16.21	0.75	0.3991
19	1720.91	16.00	0.51	0.3456
20	1748.99	14.64	0.99	0.3962
21	1855.29	10.19	2.90	0.4225
22	1749.57	15.20	0.74	0.4183
23	1800.68	16.85	0.85	0.3895
24	1734.54	19.77	0.48	0.3762
25	1799.32	20.41	0.83	0.3944

4.2. Sensibility Analysis of Factors

4.2.1. Density

We averaged the severe test of each factor, as shown in Table 5. The range of corresponding influencing factors can be obtained through the difference of the average values of five levels of different factors. As shown in Table 4, the range of Portland cement/gypsum was the largest, followed by filling materials/bonding materials, and the range of mica powder/standard sand and silicone oil content was close. To some extent, it can be explained that the factor of Portland cement/gypsum was sensitive to the parameter of sample density and was the main control factor. On the other hand, the proportion of filling material can be appropriately increased or the proportion of silicone oil can be reduced to increase the density of the sample.

Table 5. Range analysis of density kg/m^3.

Level	Mica Powder/Standard Sand	Filling Material/Bonding Material	Portland Cement/Gypsum	Silicone Oil Ratio
1	1773.84	1794.81	1724.40	1781.84
2	1753.42	1780.06	1765.39	1769.56
3	1752.51	1768.76	1735.54	1765.40
4	1765.43	1735.77	1805.29	1752.86
5	1787.88	1753.68	1802.46	1763.41
Range	35.37	59.03	80.89	28.98

4.2.2. Porosity

Although there is a close relationship between material density and porosity, there were some differences in the sensitivity of different levels of indicators to density and porosity in the orthogonal test. In this study, the porosity sensitivity analysis of materials was to ensure the compactness of similar materials with low strength and a high similarity ratio, which will affect the construction of physical similarity simulation model in the later stage. Through the sensitivity analysis of density and porosity, the effects of different levels and factors of similar materials on the differences of rock density and porosity were compared, so as to provide more scientific guidance for determining the effective material ratio.

The data processing method of the porosity test results was the same as that in Section 4.2.1. As shown in Table 6, the range of filling material/bonding material was the largest, followed by Portland cement/gypsum, and the range of silicone oil content was the smallest. The range analysis showed that the filling material/bonding material was the main factor to control the porosity. The higher the content of bonding material, the smaller the porosity of the sample. The analysis was because the fineness of the bonding material was larger than that of the filling material, which can fill the gap between standard sand, resulting in the reduction of porosity. Meanwhile, the higher the content of Portland cement in the same amount of bonding material, the smaller the porosity of the sample. This was because the cementation strength of Portland cement was stronger than that of gypsum, which can effectively gel all kinds of raw materials and form small porosity.

4.2.3. Compressive Strength

The range analysis results of compressive strength are shown in Table 7. According to Table 7, the range from large to small is the proportion of Portland cement/gypsum, filling material/bonding material, mica powder/standard sand, and silicone oil. It indicates that Portland cement/gypsum was the main factor controlling the compressive strength. Portland cement/gypsum and filling material/bonding material had a great influence on the compressive strength of the sample, and the influence degree was similar. The mica powder/standard sand and silicone oil ratio had little effect on the compressive strength of the samples, and the influence degree was similar.

Table 6. Range analysis of density %.

Level	Mica Powder/Standard Sand	Filling Material/Bonding Material	Portland Cement/Gypsum	Silicone Oil Ratio
1	15.05	12.84	16.48	14.20
2	15.10	13.44	16.36	15.51
3	15.01	15.61	15.71	16.51
4	13.73	16.31	14.13	14.42
5	16.48	17.18	12.70	14.65
Range	2.75	4.34	3.77	2.32

Table 7. Range analysis of compressive strength MPa.

Level	Mica powder/Standard Sand	Filling Material/Bonding Material	Portland Cement/Gypsum	Silicone Oil Ratio
1	0.78	1.39	0.55	0.79
2	0.77	1.07	0.65	0.97
3	0.91	0.98	0.89	0.90
4	1.23	0.56	1.22	1.18
5	1.16	0.85	1.53	1.02
Range	0.45	0.83	0.98	0.39

4.2.4. Elastic Modulus

The range analysis of elastic modulus is shown in Table 8. The range from large to small is silicone oil ratio, Portland cement/gypsum, filling material/bonding material, mica powder/standard sand. Among them, the influence of silicone oil ratio on the elastic modulus of the sample was very obvious. On the premise of keeping the proportion of raw materials of other similar materials unchanged, the elastic modulus of the sample can be effectively enhanced by increasing the silicone oil ratio. Changing the three factors of Portland cement/gypsum, filling material/bonding material, and mica powder/standard sand had little influence on the change of cohesion, and the influence degree was similar.

Table 8. Range analysis of elastic modulus GPa.

Level	Mica Powder/Standard Sand	Filling Material/Bonding Material	Portland Cement/Gypsum	Silicone Oil Ratio
1	0.3912	0.3961	0.3729	0.3823
2	0.3824	0.4192	0.3713	0.3176
3	0.4018	0.4038	0.4184	0.4830
4	0.4011	0.3763	0.4012	0.4002
5	0.4000	0.3807	0.4131	0.3877
Range	0.0204	0.0431	0.0468	0.1650

4.3. Significance Analysis

SPSS software was used to test the significance of multivariate linear regression [35,36]. Design statistical verification value is $0.05 < f < 0.10$, and the analysis results are shown in Table 9.

According to Table 9, the ratios of Portland cement/gypsum and filling material/bonding material were two important factors controlling sample density and porosity, and both were positively and negatively correlated. For compressive strength, the standardized coefficients of the four factors were similar, and their effects were positively correlated. The ratio of mica powder to standard sand had little effect on the elastic modulus, and the other three factors had similar effects on the elastic modulus. Through SPSS significance analysis, it was found that the calculation results were the same as those of factor sensitivity analysis.

Table 9. Multivariate significance analysis.

Parameter	Mica Powder/Standard Sand	Filling Material/Bonding Material	Portland Cement/Gypsum	Silicone Oil Ratio/%
Density	0.128	−0.404	0.612	−0.171
Porosity	0.080	0.624	−0.548	0.006
Compressive strength	0.154	0.057	0.001	0.005
Elastic modulus	0.166	−0.344	0.459	0.316

4.4. Parameter Determination

According to the value range of each physical parameter in Table 1, the proportion scheme of similar materials of each ore and rock of multi-layer deposit was determined, as shown in Table 10. Samples of similar materials were prepared according to the reference ratio, and the physical and mechanical indexes of three groups of reference groups were measured by the same method. The test results are shown in Table 11.

Table 10. Proportioning scheme of similar material.

Rock Formation	Mica Powder/Standard Sand	Filling Material/Bonding Material	Portland Cement/Gypsum	Silicone Oil Ratio/%
Siliceous shale	0.75	8:1	3:7	7.5
Vanadium-bearing shale	0	9:1	6:4	7.5
Carbonaceous shale	0.25	10:1	3:7	2.5

Table 11. Similar material selection and mechanical parameters.

Rock Formation	ρ /(kg/m^3)	σc /MPa	σt /kPa	n /%	E /GPa	ν	c /kPa	ϕ /(°)
Siliceous shale	1704.41	0.75	114.87	16.21	0.3991	0.2133	71.218	41.087
Vanadium-bearing shale	1661.74	0.51	84.01	14.46	0.3944	0.2100	61.891	40.275
Carbonaceous shale	1620.98	0.33	49.42	18.56	0.3368	0.2033	56.748	40.106

After calculation, the actual similarity constants of similar materials are shown in Table 12. The determined similar materials had a relatively dense structure and small porosity. The similar constants of similar materials met the requirements of test similar conditions, and the error range was less than 1.62%, which met the requirements of mineral and rock materials of similar multi-layer shale deposits.

Table 12. Similar constants of similar materials.

Rock Formation	Density	Compressive Strength	Tensile Strength	Elastic Modulus	Poisson's Ratio	Cohesion Internal	Friction Angle	$C_\sigma/(C_\rho C_l)$
Siliceous shale	1.505	150.173	150.0827	149.837	0.985	150.243	0.998	1.0020 ≈ 1
Vanadium-bearing shale	1.494	150.373	149.5060	149.087	1.000	150.264	1.003	1.0003 ≈ 1
Carbonaceous shale	1.499	149.848	150.1416	150.831	0.984	149.785	0.997	0.9935 ≈ 1

5. Discussion

The experimental results briefly presented above show the complex behavior of this like-rock. Since the primary motivation for this study was a similar material with high similarity ratio and low strength, we focused our discussion principally on the mechanisms controlling the compressive behavior of this rock-type. Other mechanical parameters, such as tensile strength, Poisson's ratio, and internal friction angle, are not discussed separately in the significance analysis because the difference interval was small. In the discussion, we supplemented the above-described laboratory programmer with some other tests that were performed to check different hypotheses.

5.1. Parameters' Selection of Range Analysis

In this study, the physical and mechanical parameters of the rock mainly included compressive strength, tensile strength, elastic modulus, internal friction angle, cohesion, and Poisson's ratio. On the one hand, considering the characteristics of large-scale, low-strength similar materials to be constructed in the study, selecting similar materials with good compactness and suitable strength conditions was the first point to be considered in the study. On the other hand, due to the small differences in tensile strength, cohesion, internal friction angle, and Poisson's ratio of samples of similar materials, the effects of various factors on the physical and mechanical parameters of samples were similar in range analysis. Taking Poisson's ratio as an example, the range analysis of different factors and levels is shown in Table 13.

Table 13. Range analysis of Poisson's ratio.

Level	Mica Powder/Standard Sand	Filling Material/Bonding Material	Portland Cement/Gypsum	Silicone Oil Ratio
1	0.2114	0.2128	0.2076	0.2097
2	0.2088	0.2147	0.2104	0.2111
3	0.2128	0.2137	0.2126	0.2125
4	0.2146	0.2078	0.2147	0.2140
5	0.2126	0.2114	0.2151	0.2130
Range	0.0058	0.0069	0.0075	0.0043

Consequently, in the analysis of test results, four parameters were selected, which were density, porosity, compressive strength, and elastic modulus.

5.2. Multivariate Linear Regression Analysis

Assuming that mica powder/standard sand is x_1, filling material/bonding material is x_2, Portland cement/gypsum is x_3, and silicone oil ratio is x_4, multiple linear regression analysis [37,38] was carried out on the density, porosity, compressive strength, and elastic modulus controlled by these four factors, and the regression equation can be obtained as follows.

$$y_i = B_{0,i} + B_{1,i}x_1 + B_{2,i}x_2 + B_{3,i}x_3 + B_{4,i}x_4 \tag{1}$$

where y_i is the physical and mechanical parameters of similar material samples. $B_{0,i}$, $B_{1,i}$, $B_{2,i}$, $B_{3,i}$, and $B_{4,i}$ are linear regression coefficients, and i is 1~4, representing density, porosity, compressive strength, and elastic modulus in turn.

The regression coefficients corresponding to each physical and mechanical parameter were obtained by SPSS, as shown in Table 14. The residual independence of linear regression data was tested by the Durbin Watson correlation coefficient, as shown in Table 15.

Table 14. Coefficients of multivariate linear regression analysis.

i	$B_{0,i}$	$B_{1,i}$	$B_{2,i}$	$B_{3,i}$	$B_{4,i}$
1	1822.953	16.039	−12.654	40.124	−2.142
2	8.076	0.594	1.156	−2.127	−0.004
3	1.233	0.484	−0.159	0.533	0.027
4	0.409	0.014	−0.007	0.021	0.003

Table 15. Durbin Watson coefficient of multiple linear regression analysis.

Parameter	Density	Porosity	Compressive Strength	Elastic Modulus
Durbin Watson	2.3326	1.2580	2.3932	2.6805

Meanwhile, outlier detection was detected for the test results, as shown in Figure 4. Different physical and mechanical parameters had an outlier in different groups (box in

Figure 2). The existence of outliers will lead to a certain deviation in the value of the linear regression coefficients [39,40]. It was necessary to remove outliers and recalculate multiple regression coefficients [41]. The regression coefficients corresponding to each physical and mechanical parameter with outliers removed are summarized in Table 12.

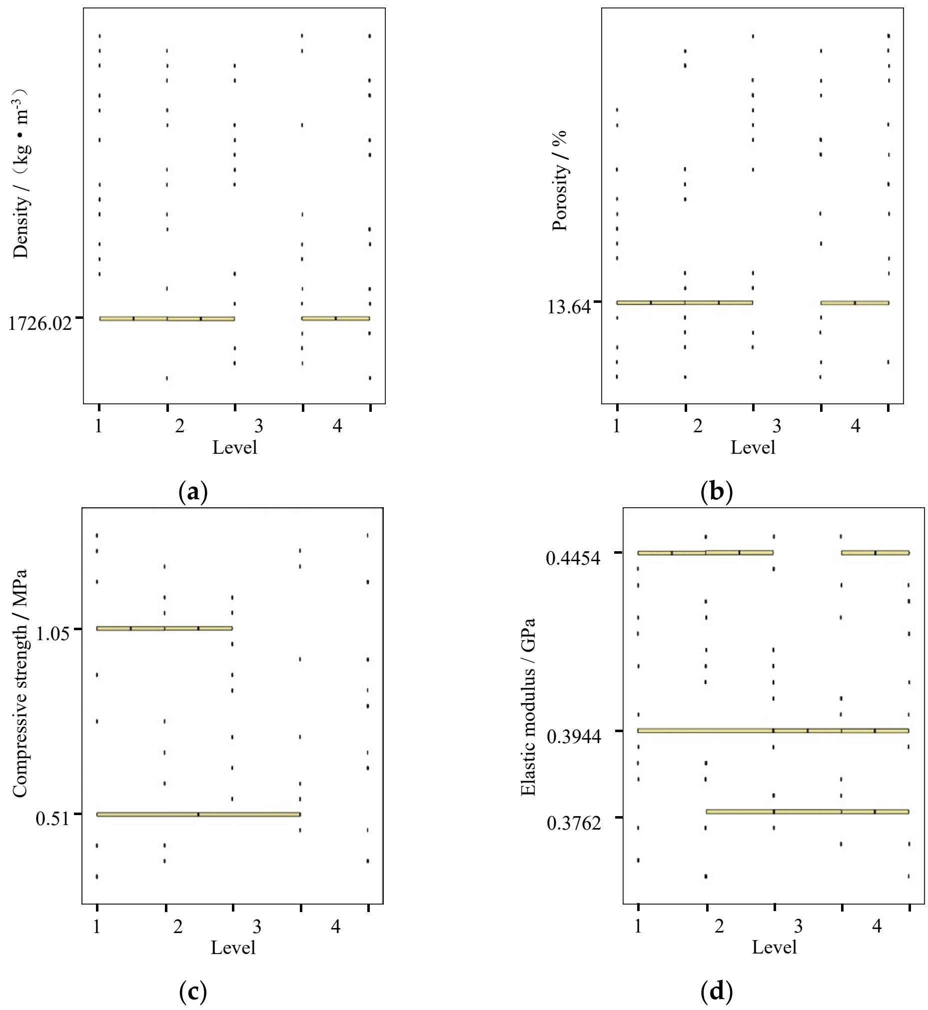

Figure 4. Outlier detection for test results. (**a**) Density. (**b**) Porosity. (**c**) Compressive strength. (**d**) Elastic modulus.

Through multiple linear regression analysis of the Durbin Watson correlation coefficient [42] (Tables 16 and 17), it was determined that the residual was independent. Meanwhile, the more uncorrelated the residual terms of each parameter after correction (excluding outliers).

Table 16. Coefficients of multivariate linear regression analysis (excluding abnormal points).

i	$B_{0,i}$	$B_{1,i}$	$B_{2,i}$	$B_{3,i}$	$B_{4,i}$
1	1831.861	12.791	−13.466	39.461	−1.817
2	7.888	0.594	1.181	−2.117	−0.014
3	1.299	0.425	−0.166	0.538	0.036
4	0.380	0.024	−0.004	0.022	0.001

Table 17. Durbin Watson coefficient of multiple linear regression analysis (excluding abnormal points).

Parameter	Density	Porosity	Compressive Strength	Elastic Modulus
Durbin Watson	2.1310	1.2180	2.2600	2.0880

6. Conclusions

Using the orthogonal test method, the L25 (4^5) orthogonal design and 25 groups of similar material ratio tests were adopted, and the density test, porosity test, and compression test were carried out in this paper. The physical and mechanical indexes such as density, porosity, compressive strength, and elastic modulus of different similar material ratio tests were obtained.

The results of the similar material proportioning test showed that the physical and mechanical properties required by the prototype of the similar model were within its distribution range. Among them, the distribution range of porosity and elastic modulus of 25 groups of samples with the similar material ratios was small, and the distribution range of density and compressive strength met the requirements of the orthogonal test.

The sensitivity analysis and significance analysis of various factors by SPSS software showed that the density and compressive strength of similar materials were most affected by the ratio of Portland cement to gypsum. The porosity was most affected by the ratio of filling material to bonding material. The proportion of silicone oil was the main factor controlling the elastic modulus.

The multiple linear regression analysis of 25 groups of test results was carried out, and the optimized multiple linear regression equation was obtained through anomaly detection and anomaly elimination. According to the characteristics of the Shanghengshan multilayer deposit and the research conditions of the material model, the similar materials of siliceous shale, carbonaceous shale, and vanadium-bearing shale were determined. The selected similar materials had a relatively dense structure and small porosity, and their main physical and mechanical properties were similar to those of the simulated multi-layer vanadium-bearing shale. Among them, the error between the actual similarity constant and the design value of similar materials was less than 1.62%, which met the requirements of test similarity conditions and can meet the requirements of simulated shale. The selection of similar materials is feasible.

Author Contributions: Conceptualization, Y.Y., Y.S., and X.W.; methodology, N.H., Y.Y., and Y.S.; software, Y.S. and X.H.; validation, Y.S. and X.H.; formal analysis, N.H., Y.Y., and Y.S.; investigation, N.H. and Y.S.; resources, Y.Y. and N.H.; data curation, Y.S. and X.H.; writing—original draft preparation, Y.S., Y.Y., and N.H.; writing—review and editing, N.H., Y.S., and Y.Y.; visualization, Y.S.; supervision, N.H. and Y.Y.; project administration, Y.Y. and X.W.; funding acquisition, Y.Y. and Y.S. All authors have read and agreed to the published version of the manuscript.

Funding: This research was funded by the Natural Science Foundation of Hubei Province (No. 2020CFB123), Scientific Research Project of Hubei Provincial Department of Education (No. Q20201109), Key Research and Development Plan of Hubei Province (No. 2020BCA082), and Innovation and entrepreneurship training program for college students of WUST (No. 20ZB012).

Institutional Review Board Statement: Not applicable.

Informed Consent Statement: Not applicable.

Data Availability Statement: All data are presented in this article in the form of figures and tables.

Conflicts of Interest: The authors declare no conflict of interest.

References

1. Fu, J.H.; Sun, H.T.; Wen, G.C.; Li, R.F.; Tao, Z.G. Three-Dimensional Physical Similarity Simulation of the Deformation and Failure of a Gas Extraction Surface Well in a Mining Area. *Adv. Civ. Eng.* **2020**, *10*, 8834199. [CrossRef]
2. Chen, F.; Kusaka, H.; Bornstein, R.; Ching, J.; Grimmond, C.S.B.; Grossman-Clarke, S.; Zhang, C. The integrated WRF/urban modelling system: Development, evaluation, and applications to urban environmental problems. *Int. J. Climatol.* **2011**, *31*, 273–288. [CrossRef]
3. Ren, W.; Guo, C.; Peng, Z.; Wang, Y. Model experimental research on deformation and subsidence characteristics of ground and wall rock due to mining under thick overlying terrane. *Int. J. Rock Mech. Min. Sci.* **2010**, *47*, 614–624. [CrossRef]
4. Wen, C.X.; Jia, S.P.; Fu, X.F.; Meng, L.D.; Zhao, Z.Y.; Riccio, A. Experimental Research and Sensitivity Analysis of Mudstone Similar Materials Based on Orthogonal Design. *Adv. Mater. Sci. Eng.* **2020**, *9*, 2031276. [CrossRef]
5. Shi, X.M.; Liu, B.G.; Xiang, Y.Y.; Qi, Y. A Method for Selecting Similar Materials for Rocks in Scaled Physical Modeling Tests. *J. Min. Sci.* **2018**, *54*, 938–948. [CrossRef]
6. Cai, Z.Q.; Li, X.Y.; Lei, B.; Yuan, J.F.; Hong, C.S.; Wang, H. Laboratory Experimental Laws for the Radon Exhalation of Similar Uranium Samples with Low-Frequency Vibrations. *Sustainability* **2018**, *10*, 2937. [CrossRef]
7. Zhang, Y.N.; Deng, H.W.; Deng, J.R.; Liu, C.J.; Ke, B. Peridynamics simulation of crack propagation of ring-shaped specimen like rock under dynamic loading. *Int. J. Rock Mech. Min. Sci.* **2019**, *123*, 104093. [CrossRef]
8. Mou, Y.Z.; Zhou, C.B.; Jiang, N.; Xiao, W.F.; Du, C.F.; Meng, X.Z. Experiment Study on Proportioning of Similar Materials in Weak Surrounding Rocks of Rich-Water Faults. *Geotech. Geol. Eng.* **2020**, *38*, 3415–3433. [CrossRef]
9. Ye, Y.C.; Shi, Y.B.; Wang, Q.H.; Yao, N.; Lu, F.; Yue, Z. Test model research on low strength similar material of Shanghengshan multilayer shale deposit. *Rock Soil Mech.* **2014**, *35*, 114–120.
10. Xu, X.L.; Chen, L.; Zhu, X.W. Study on the Fractal Dimension of Rock Fracture Surface after Different Temperatures. *Appl. Mech. Mater.* **2015**, *751*, 164–169. [CrossRef]
11. Cheng, W.M.; Sun, L.L.; Wang, G.; Du, W.Z.; Qu, H.Y. Experimental research on coal seam similar material proportion and its application. *Int. J. Min. Sci. Technol.* **2016**, *26*, 913–918. [CrossRef]
12. Xu, Z.L.; Luo, Y.B.; Chen, J.X.; Su, Z.M.; Zhu, T.T.; Yuan, J.P. Mechanical properties and reasonable proportioning of similar materials in physical model test of tunnel lining cracking. *Constr. Build. Mater.* **2021**, *300*, 123960. [CrossRef]
13. Fu, H.Y.; Qi, S.X.; Shi, Z.N.; Zeng, L.; Lu, G.Y. Mixing Ratios and Cementing Mechanism of Similar Silty Mudstone Materials for Model Tests. *Adv. Civ. Eng.* **2021**, *2021*, 2426130. [CrossRef]
14. Sun, P.; Sun, H.T.; Lin, F.J.; Yang, X.L.; Jiang, W.G.; Wu, W.B.; Jia, Q.M. Experimental study on the ratio model of similar materials in the simulation test of coal and gas outburst. *Sci. Rep.* **2021**, *11*, 1–14.
15. Wallace, C.S.; Schaefer, L.N.; Villeneuve, M.C. Material Properties and Triggering Mechanisms of an Andesitic Lava Dome Collapse at Shiveluch Volcano, Kamchatka, Russia, Revealed Using the Finite Element Method. *Rock Mech. Rock Eng.* **2021**, *2021*, 1–18.
16. Gu, D.M.; Huang, D. A complex rock topple-rock slide failure of an anaclinal rock slope in the Wu Gorge, Yangtze River, China. *Eng. Geol.* **2016**, *208*, 165–180. [CrossRef]
17. Arora, K.; Gutierrez, M. Viscous-elastic-plastic response of tunnels in squeezing ground conditions: Analytical modeling and experimental validation. *Int. J. Rock Mech. Min. Sci.* **2021**, *146*, 104888. [CrossRef]
18. Fan, Q.X.; Zhang, Q.Q.; Liu, G.R. A Stress Analysis of a Conical Pick by Establishing a 3D ES-FEM Model and Using Experimental Measured Forces. *Appl. Sci.* **2019**, *9*, 9245410. [CrossRef]
19. Yang, M.Z.; Yang, Y.; Zhao, B.; Nascimbene, R. Study on the Proportion of Conglomerate Similar Materials Based on the Orthogonal Test. *Shock Vib.* **2021**, *2021*, 6657323.
20. Cheng, X.Y. Damage and failure characteristics of rock similar materials with pre-existing cracks. *Int. J. Coal Sci. Technol.* **2019**, *6*, 505–517. [CrossRef]
21. Ye, Y.C.; Shi, Y.B.; Wang, Q.H.; Liu, Y.Z.; Yao, N.; Lu, F. Experimental study of deformation of wall rock and stoping sequence in mining gently inclined and multilayer deposits by backfill mining in Shanghengshan. *J. Min. Saf. Eng.* **2015**, *32*, 407–413.
22. Song, H.Y.; Shi, H.Z.; Li, G.S.; Ji, Z.S.; Li, S.W.; Liu, C.G.; Li, X.J. Three-Dimensional Numerical Simulation of Energy Transfer Efficiency and Rock Damage in Percussive Drilling With Multiple-Button Bit. *J. Energy Resour. Technol.* **2021**, *143*, 024501. [CrossRef]
23. Danilov, V.; Ayzenshtadt, A.; Frolova, M. Practical Application of the Similarity Law of Structures in the Reconstruction of the Surface Layer of Bricks. *Mater. Sci. Forum* **2021**, *1017*, 21–30. [CrossRef]
24. Yang, G.X.; Qi, S.W.; Wu, F.Q.; Zhan, Z.F. Seismic amplification of the anti-dip rock slope and deformation characteristics: A large-scale shaking table test. *Soil Dyn. Earthq. Eng.* **2018**, *115*, 907–916. [CrossRef]
25. Cui, F.; Jia, C.; Lai, X.P. Study on Deformation and Energy Release Characteristics of Overlying Strata under Different Mining Sequence in Close Coal Seam Group Based on Similar Material Simulation. *Energies* **2019**, *12*, 4485. [CrossRef]
26. Bai, J.W.; Feng, G.R.; Wang, Z.H.; Wang, S.Y.; Qi, T.Y.; Wang, P.F. Experimental Investigations on the Progressive Failure Characteristics of a Sandwiched Coal-Rock System Under Uniaxial Compression. *Appl. Sci.* **2019**, *9*, 1195. [CrossRef]
27. Urszula, K.; Jan, B.; Justyna, G.Z. Multi-Criteria Analysis of Potential Applications of Waste from Rock Minerals Mining. *Appl. Sci.* **2019**, *9*, 441.

28. Jiao, P.F.; Zhang, X.; Li, X.Z.; Liu, B.H.; Zhang, H.J.; Zhou, Y.X. Experimental Study on the Ratio of Similar Materials in Weak Surrounding Rock Based on Orthogonal Design. *J. Eng.* **2018**, *2018*, 2591758. [CrossRef]
29. Chen, S.J.; Wang, H.L.; Zhang, J.W.; Xing, H.L.; Wang, H.Y.; Lv, G.C. Experimental Study on Low-Strength Similar-Material Proportioning and Properties for Coal Mining. *Adv. Mater. Sci. Eng.* **2015**, *2015*, 696501. [CrossRef]
30. Li, J.G.; Wu, Y.; Wang, Y.Y.; Qin, N.; Wang, W.X. Experimental Study on Self-Made Similar Material of Soft Rock. *Key Eng. Mater.* **2017**, *717*, 140–146. [CrossRef]
31. Lin, M.Q.; Zhang, L.; Liu, X.Q.; Xia, Y.Y.; He, J.Q.; Ke, X.S.; Vipulanandan, C. The Meso-Analysis of the Rock-Burst Debris of Rock Similar Material Based on SEM. *Adv. Civ. Eng.* **2020**, *717*, 140–146. [CrossRef]
32. Ko, T.Y.; Lee, S.S. Characteristics of Crack Growth in Rock-Like Materials under Monotonic and Cyclic Loading Conditions. *Appl. Sci.* **2020**, *10*, 719. [CrossRef]
33. China Academy of Building Sciences. *Provisions of Test Method for Mechanical Properties of Ordinary Concrete (GB/T 50081-2002)*; China Construction Industry Press: Beijing, China, 2003; pp. 11–36.
34. Changjiang Academy of Sciences, Changjiang Water Resources Commission. *Code for Rock Test of Water Resources and Hydropower Engineering (SL264-2001)*; China Water Resources and Hydropower Press: Beijing, China, 2001; pp. 10–16.
35. Cao, Y.R. Analysis and implementation of virtual variable regression in SPSS. *Stat. Decis.* **2018**, *34*, 66–69.
36. Chen, H.B.; Wang, B.B.; Zhou, J.C. The Prediction Model of the Correction Coefficient of Concrete Strength is Tested based on the Method of SPSS Regression Analysis. *Front. Sci. Eng.* **2021**, *1*, 110–112.
37. Ameloko, A.A.; Ayolabi, E.A.; Okezie, U. Modeling groundwater total dissolved solid from derived electromagnetic data using multiple linear regression analysis: A case study of groundwater contamination. *Model. Earth Syst. Environ.* **2020**, *6*, 1863–1875.
38. Ning, Y.S.; He, S.; Wu, Z.Y.; Xing, C.X.; Zhang, L. A Review of Deep Learning Based Speech Synthesis. *Appl. Sci.* **2019**, *9*, 4050. [CrossRef]
39. Peixoto, S.F.; Horbe, A.M.C.; Soares, T.M.; Freitas, C.A.; de Sousa, E.M.D.; de Figueiredo Iza, E.R.H. Boolean and fuzzy logic operators and multivariate linear regression applied to airborne gamma-ray spectrometry data for regolith mapping in granite-greenstone terrain in Midwest Brazil. *J. S. Am. Earth Sci.* **2021**, *112*, 103562. [CrossRef]
40. Jin, J.; Fang, H.; Daly, I.; Xiao, R.C.; Miao, Y.Y.; Wang, X.Y.; Cichocki, A. Optimization of Model Training Based on Iterative Minimum Covariance Determinant in Motor-Imagery BCI. *Int. J. Neural Syst.* **2021**, *31*, 2150030. [CrossRef]
41. Magdalena, H.; Mariusz, M. Object Retrieval in Microscopic Images of Rocks Using the Query by Sketch Method. *Appl. Sci.* **2019**, *10*, 278.
42. Kabaila, P.; Farchione, D.; Alhelli, S.; Bragg, N. The effect of a Durbin–Watson pretest on confidence intervals in regression. *Stat. Neerl.* **2020**, *75*, 4–23. [CrossRef]